Science Press

Trans. Nonferrous Met. Soc. China 17(2007) s680−s684

Transactions of Nonferrous Metals Society of China

www.csu.edu.cn/ysxb/

Electro-magnetism of peg-20000 doped with nano-cobalt ferrite oxide powder containing La^{3+}

XIAO Li(肖　利)[1, 2], FANG Zheng(方　正)[2], QIU Guan-zhou(邱冠周)[3], LIU Jian-she(柳建设)[3]

1. Hunan Metallurgic Professional Technical College, Zhuzhou 412000, China;
2. School of Chemistry and Chemical engineering, Central South University, Changsha 410083, China;
3. School of Resources Processing and Bioengineering, Central South University, Changsha 410083,China

Received 15 July 2007; accepted 10 September 2007

Abstract: The sol-gel method was used to prepare three kinds of nanometer magnetic particles, such as the nano-cobalt ferrite oxide powders and those doped by $LaCl_3 \cdot nH_2O$. In the thermo-decomposition process of the precursors to get these magnetic particles, TG/DTG was applied to investigate their character. The prepared magnetic particles with average diameter less than 100 nm were characterized by XRD and TEM. The results show the difference between the activation energies of these particles in different thermo-decomposition stages, even not in the same stage for different samples. The cobalt ferrite doped with La^{3+} affects its saturation magnetization(m_s) and coercive force(H_c). As $CoCl_2 \cdot 6H_2O$ is partly substituted by La^{3+}, the value of H_c decrease with the increase of m_s. When $FeCl_2 \cdot 4H_2O$ is partly substituted by La^{3+}, H_c increases obviously. The three kinds of nanometer magnetic particles were doped into polyethylene glycol-20000 (peg-20000) with different ratios respectively to obtain compound substance with optimal conductivity of 0.686 S/m.

Key words: nanometer particle; thermo-decomposition process; magnetism; conductivity; polymer films

1 Introduction

Chemical world is concentrating on improving the properties of some polymers film[1−3], and many novel electrical, magnetic, and optical properties of nanometer particles have also been investigated recently[4]. Among these researches, it is found that the polymers doped with nanometer particles can improve some performance. WANG et al[5] have reported that the polymer could be used as wave-absorbing materials when the magnetic nano- particles were doped into polymer electrolyte.

As is well known, the cobalt ferrite, $CoFe_2O_4$, is a type of hard magnetic material, which possesses high coercive force and moderate saturation magnetization as well as remarkable chemical stability and mechanical hardness. The rare earth elements can improve the magnetic conductivity performance of the magnetic oxide particles[6]. It has been studied that the magnetism of $CoFe_2O_4$ will change when transition metal ions are doped[7], especially, Yb^{3+}, La^{3+} can lead to lattice distorting and to intensify its magneto-optic effect[8].

Strong efforts are currently devoted to studying magnetic properties and microstructure of polymer electrolytes film doped with nano-particles [9-10], there are few reports about the changes of its electro-conductivity.

In this study, the preparation and the characterization of magnetic nanometer powders of cobalt ferrite and those doped by $LaCl_3.nH_2O$ with different mole ratios are reported. The activation energy in every thermal decomposition stage of the precursors to get these nano-oxides, is calculated. The electro-conductivity of magnetic nano-particles doping into the polyethylene glycol-20000 (abridging peg-20000) polymer film, is studied.

2 Experimental

2.1 Preparation of nanometer $CoFe_2O_4$ and doping with La^{3+}

The nanometer $CoFe_2O_4$ was prepared by a sol-gel method. The constant mole ratio of $CoCl_2 \cdot 6H_2O$ and

Foundation item: Project (50374077) supported by the National Science Foundation of China; Project (07D069) supported by the Education Department Foundation of Hunan Province, China
Corresponding author: QIU Guan-zhou; E-mail: xiaoli_csu@163.com

$FeCl_2 \cdot 4H_2O$ and a fixed amount of citric acid were mixed with small quantity of water under magnetic stir for about 1 h up to the mixture turned to red sol. A little peg and absolute alcohol was added into the sol to dilute it until the total metal ion concentration was 0.1 mol/L under continuous stir for 2 h, and treated under ultrasonic condition for 0.5 h to obtain uniform solution, and then evaporated under 343 K to get a puce gel. The gel was dried under infrared light. The finally obtained solid was milled and burned at 773 K for 3 h to get the magnetic ferrite oxide $CoFe_2O_4$ particles named as sample 1.

Only changed the ratio of the two metal chlorides to acquire different formulas for magnetic ferrite oxide particles using the same process mentioned above. First, fixed amount of $FeCl_2 \cdot 4H_2O$, $CoCl_2 \cdot 6H_2O$ was replaced by 90% $CoCl_2 \cdot 6H_2O$ and 10% $LaCl_3 \cdot nH_2O$, and second, fixed amount of $CoCl_2 \cdot 6H_2O$, $FeCl_2 \cdot 4H_2O$ was replaced by 90% $FeCl_2 \cdot 4H_2O$ and 10% $LaCl_3 \cdot nH_2O$ to obtain two types of $CoFe_2O_4$ containing La^{3+}, which were named as sample 2 and sample 3, respectively.

2.2 Analysis and characterization

Mettler Toledo TG/DTG analytic apparatus at flow air atmosphere of 25mL/s, with constant rising rate of temperature 10 K/mim, ranging from 298 K to 1 273 K, was used for the thermo-decomposition of precursors. A Siemens D500 X-ray diffractometer with Cu K_α radiation, working voltage and current of 40 kV and 20 mA, respectively, was used for the nano-oxides. The morphology and size of the synthesized particles were observed through a Philips CM12 TEM operated at 175 kV. And the magnetism was measured by LDJ9600−1 vibration sample magnetometer.

2.3 Doping of oxides into peg-20000 and its electro-chemical testing

Three types of nano-cobalt ferrite oxide particles, samples 1, 2 and 3 , were doped into peg-20000, respectively, the contents of each oxide of 5%, 10%, 15% and 20% (mass ratio), respectively. Each of the compounds was pressed to form a uniform film with a certain thickness. Their specific volume conductance, δ_v was measured by CHI660B electro-chemistry work station with frequency of 10^{-2}−10^5 Hz and AC voltage up to 5 mV.

3 Results and discussion

3.1 Analysis of thermo-decomposition process of precursors

The report on the thermal decomposition course of dried gel is few due to its complex composition.

Figs.1−3 shows the TG/DTG curves of the precursors of three kinds of cobalt ferrite oxides. Four obvious peaks appear in the DTG curves of Figs.1 and 3, and five visible peaks appear in Fig.2. Each of these peaks corresponds to a thermo-composition stage. Combining with gravity loss peak in TG curves, we can see from Figs.1 and 3 that mostly gravity loss was due to movement of crystal water in the first stage, due to free citric acid decomposition in the second stage, due to decomposition of citrate coordinated to metallic ion in

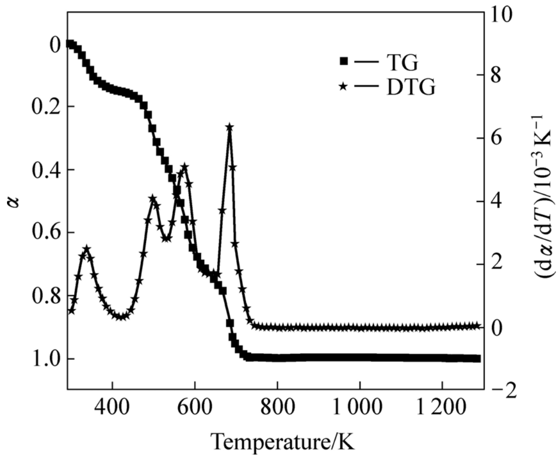

Fig.1 TG/DTG curves of precursor sample 1

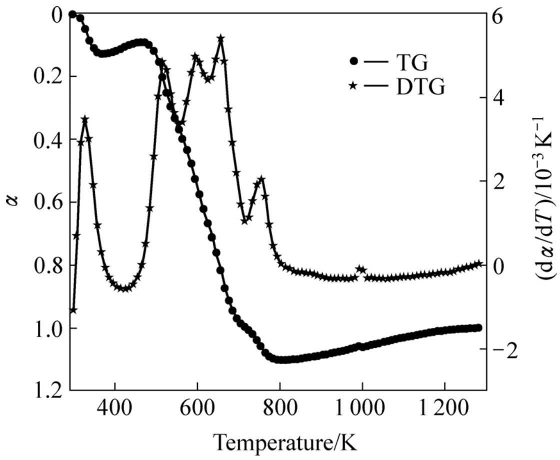

Fig.2 TG/DTG curves of precursor sample 2

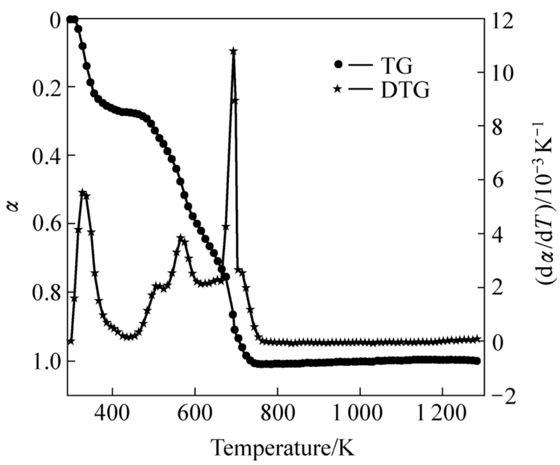

Fig.3 TG/DTG curves of precursor sample 3

the third stage, and due to citrate break up and spinal crystal formation in the final stage. In Fig.2, when the temperature was over about 650 K, the two peaks were present corresponding to the final stage. After 800 K, the TG curve somewhat rises in Fig.2, which shows that the micro-content alloy might produce, resulting in MASS increase[8].

The dynamics equation of solid thermo-decomposition is often expressed as[11]

$$d\alpha / dt = k(T) f(\alpha) = A[\exp(-E / RT)](1-\alpha)^n \quad (1)$$

where n is reaction order and α is reaction extent of sample at a certain time. α is defined as $\alpha = (m_0 - m_t)/(m_0 - m_\infty)$, where m_0, m_∞ and m_t are the mass of sample before and after reaction and at t=t_r respectively. Under a certain heating rate, $\beta = dT / dt$, we have

$$d\alpha / dT = (A/\beta)(1-\alpha)^n \exp(-E/RT) \quad (2)$$

Taking logarithm of Eqn.(2), we have

$$\ln(d\alpha / dT) = \ln[(A/\beta)(1-\alpha)^n] - E/RT \quad (3)$$

Plotting ln(dα/dT) vs 1/T, the activation energy E can be obtained from the slope. The activation energy data for every stage of thermo-decomposition are listed in Table 1.

It can be seen that the activation energies of the three samples are different in each stage, not even in the same stage for different samples. This can be explained by the fact that the doping of $LaCl_3 \cdot nH_2O$ changes in the interaction between Co^{2+}, Fe^{3+} and citric ions, and makes precursors complicate.

Table 1 Thermo-decomposition activation energy (AE) of three precursors samples in different stages (kJ/mol)

Stage	Sample 1	Sample 2	Sample 3
Ⅰ	29.97	14.23	78.49
Ⅱ	66.03	88.26	79.44
Ⅲ	38.84	45.59	68.69
Ⅳ	9.56	30.69	10.76
Ⅴ	/	105.23	/

3.2 XRD analysis of particles

The samples were characterized by XRD, and the results are shown in Fig.4. It can be seen from Fig.4 that the nanometer $CoFe_2O_4$ spectra is mostly the same as that of normal spinal $CoFe_2O_4$ (PDF#22－1086), without miscellaneous phase. The spectra of the samples 2 and 3 are similar to that of nanometer $CoFe_2O_4$, but with weaker peak intensities. The order of peak intensity in the same crystal plane is as follows: sample 1＞sample 2＞sample 3, which may be because of different metallic ion radii and ratios in crystal. According to Scherrer's formula[12], the average diameters of grain size are calculated to be 40−60 nm.

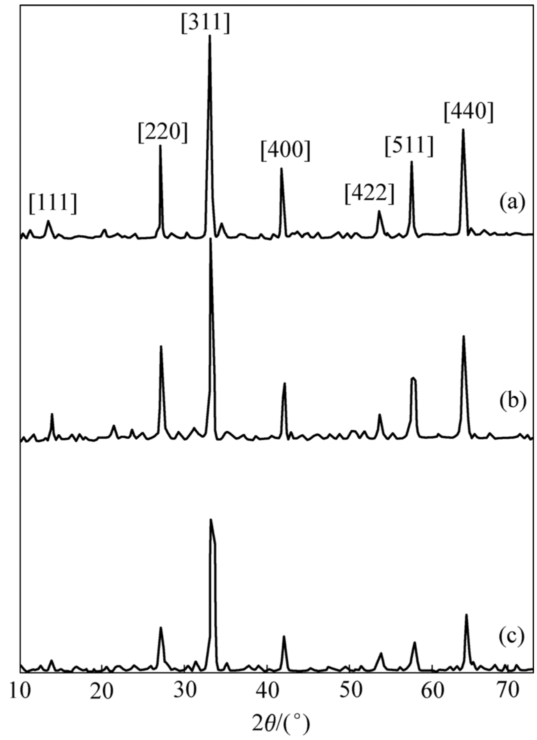

Fig.4 XRD spectra of nanometer samples: (a) Sample 1; (b) Sample 2; (c) Sample 3

3.3 TEM analysis of particles

It can be seen from Fig.5 that the average diameter of sample particles is below 100 nm but glomeration occurs owing to magnetism.

3.4 Magnetism analysis of particles

The saturation magnetization (m_s) and coercive force (H_c) of the particles measured by using vibration sample magnetometer are shown in Table 2.

Table 2 Saturation magnetizations (m_s) and coercive force (H_c) of samples

Sample No.	$m_s/(10^{-4}$ T)	H_c/(kA·m^{-1})
1	72	6.21
2	91	4.93
3	51	8.52

As $CoCl_2 \cdot 6H_2O$ is partly substituted of La^{3+} for sample 2, H_c decreases with the increase of m_s. Perhaps it is due to the residual charge in rare earth ion vs Co^{2+} in the crystal as well as its larger radius, which leads to an

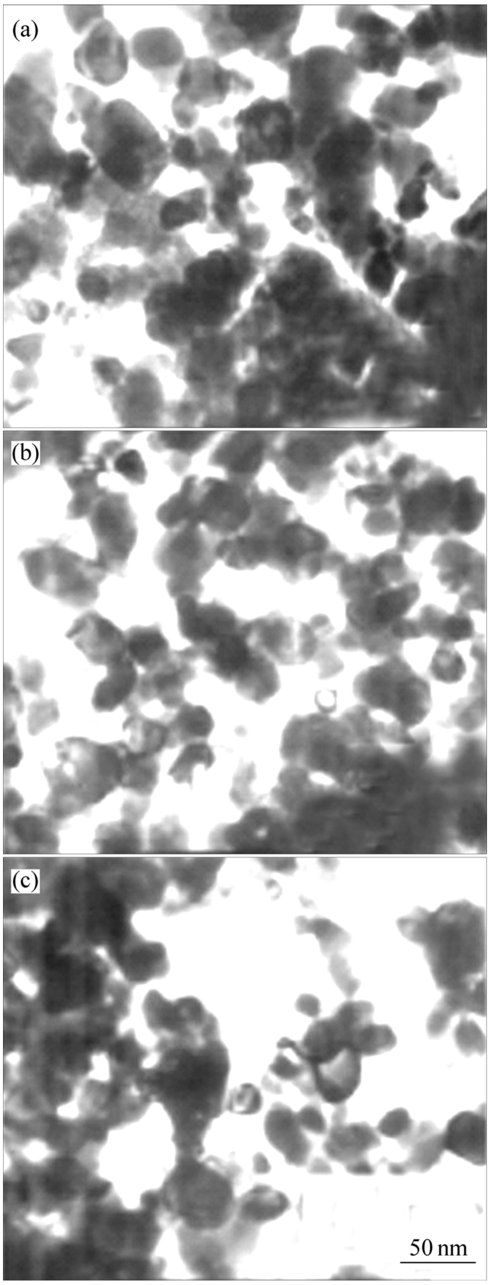

Fig.5 TEM images of samples: (a) Sample 1; (b) Sample 2; (c) Sample 3

incline of magneto-electron spin and weaken exchange couple between $Fe^{3+}$and Co^{2+}[13]. When $FeCl_2·4H_2O$ partly substitute by La^{3+}, H_c increases obviously because 4 f electronic shell of outer space in rare earth ions and spin-orbit couple contributes to the magnetic-anisotropy [14].

3.5 AC impedance analysis of polymer film of peg-20000 doped by magnetic particles

It can be seen from Table3 that the conductivity, δ_v of films first enhances and then falls down. The conductivities of three groups of the compounds all reach the maximum when the concentration doped is 10%. Among them, peg-20000 doped by sample 3 is the highest, up to 0.686 S/m. However, the conductivity drops as the concentration of the doped oxides is less or more than 10%. This can be explained by the fact that when the doped oxide in peg-20000 is less, the migratory charges supplied from the oxide are not enough, resulting in lower conductivity. In contrary, too much more doping increases in migratory charges supplied[15], which makes the charge transferring in relative narrow channels move, and jams charges flowing[16].

Table 3 Optimal conductivity of peg-20000 doped with different contents of cobalt ferrite oxide (10^{-3} $S·m^{-1}$)

Sample No.	5%	10%	15%	20%
1	0.263	0.877	0.139	0.123
2	0.802	2.96	0.846	0.081
3	19.6	686	8.54	0.302

4 Conclusions

1) When $CoCl_2·6H_2O$ or $FeCl_2·4H_2O$ in the crystal are partly substituted by La^{3+}, the activation energies of the three precursors in each of thermo-decomposition stages are different, even not in the same stage for different samples.

2) XRD peak intensify of nano-cobalt ferrite oxide and their magnetism changes as La^{3+} ions are added. The average diameter of sample particles is below 100 nm observed from TEM images but glomeration owing to magnetism. The cobalt ferrite doped with La^{3+} affects its saturation magnetization and coercive force. As $CoCl_2·6H_2O$ is partly substituted by La^{3+}, the H_c decreases with the increases of m_s. When $FeCl_2·4H_2O$ is partly substituted by La^{3+}, H_c increases obviously.

3) Peg-20000 doped by the nano-magnetic oxide particles containing less amount of La^{3+} can make its conductivity rise; the optimum value is 0.686 S/m for sample 3 in which Fe^{2+} is partly replaced by La^{3+}.

References

[1] YOON M, KIM Y, KIM Y M. Superparamagnetic properties of nickel nanoparticles in an ion-exchange polymer film[J]. Materials Chemistry and Physics, 2005, 91(1): 104−107.

[2] YOON M, KIM T M, KIM Y. Magnetic properties of iron nanoparticles in a polymer film[J]. Journal of Magnetism and Magnetic Materials, 2003, 265(2): 357−362.

[3] PARK I W, YOON M, KIM Y M. Magnetic properties and microstructure of cobalt nanoparticles in a polymer film[J]. Solid state Communications, 2003, 44(2): 385−389.

[4] HSEIH C, HUANG W, LUE J. Superparamagnetism of transition metal nanoparticles in conducting polymer film[J]. Journal of Physics

and Chemistry of Solids, 2002, 63(4): 733−776.
[5] WANG G Q, ZHANG P, YONG Z J. Microwave absorbency of polymer doped by nanometer-sized ferrite and its electromagnetic parameters[J]. Huazhong Univ of Sci & Tech, 2001, 7(1): 89−91. (in Chinese)
[6] ZHUANG J, CHEN Y, SHI J. Effect of cerium on electromagnetic properties of nanometer ferrite[J]. Journal of the Chinese Rare Earth Society, 2002, 20(5): 324−326. (in Chinese)
[7] ZHOU B, ZHANG Y, LIAO C. Magnetism and phase transition for $CoFe_{2-x}Mn_xO_4$ nanocrystalline thin films and powders[J]. Journal of Magnetism and Magnetic Materials, 2002, 247(1): 70−76.
[8] KIM W C, SAM J K, JUNG C S. Structural and magnetic properties of $CoFe_{1.9}RE_{0.1}O_4$ (RE=Yb, La) prepared by a sol-gel method[J]. Journal of Magnetism and Magnetic Materials, 2002, 242(1): 197−200.
[9] PERSI L, CORE F. Nanocomposite polymer electrolytes and their impact on the lithium battery technology[J]. Solid State Ionics, 2000, 135(1): 47−52.
[10] RAJENDRAN S, UMA T. Effect of ceramic oxide on PMMA based polymer electrolyte systems[J]. Materials Letters, 2000, 45(1): 191−196.
[11] YANG C M, FANG Z, LIU J B. A study on the kinetics of thermal decomposition of polyaniline[J]. Thermochimica Acta, 2000, 159(2): 352−353.
[12] ZHAN K T, ZHEN J, ZHANG H. Study of the synthesis, structure and magnetic properties of nanometer $BaFe_{12}O_{19}$ permanent magnetic ferrite powder[J]. Chinese Journal of Inorganic Chemistry. 2002, 18(3): 294−297. (in Chinese)
[13] NUNES A, YANG L Y. Calculated ferrite nanocrystal relaxation and its magnetic implications[J]. Surface Science, 1998, 399(2): 225−233.
[14] WIESLAW A, KACZMAR K. Structural and magnetic properties of cobalt-doped iron oxide particles prepared by novel mechanochemical method[J]. Journal of Magnetism and Magnetic Materials, 1996, 43(1): 157−158.
[15] REN X M, PICKUP P G. Impedance of polypyrrole perchlorate polypyrrole poly (styrene sulfonate) bilayers [J]. J Physchem, 1993, 97(6): 3941−3943.
[16] NIETO F J, TUCCERI R I. The effect of pH on the charge transport at redox polymer modified electrodes: An ac impedance study applied to poly (α-aminophenol) film electrodes[J]. J Electroanal Chem, 1996, 416(1): 1−24.

(Edited by LONG Huai-zhong)